

Correlation effects on the electronic structure of TiOCl: a NMTO+DMFT study

T. Saha-Dasgupta¹, A. Lichtenstein² and R. Valentí³

¹*S.N. Bose National Centre for Basic Sciences, JD Block,
Sector III, Salt Lake City, Kolkata 700098, India.*

²*Institut für Theoretische Physik, Universität Hamburg, 20355 Hamburg, Germany. and*

³*Institut für Theoretische Physik, J.W.Goethe-Universität Frankfurt, 60054 Frankfurt/Main, Germany.*

(Dated: February 2, 2008)

Using the recently developed N-th order muffin-tin orbital-based downfolding technique in combination with the Dynamical Mean Field theory, we investigate the electronic properties of the much discussed Mott insulator TiOCl in the undimerized phase. Inclusion of correlation effects through this approach provides a description of the spectral function into an upper and a lower Hubbard band with broad valence states formed out of the orbitally polarized, lower Hubbard band. We find that these results are in good agreement with recent photo-emission spectra.

Introduction -

A challenging task in the field of strongly electron-correlated materials is the description of correlation effects, within a possibly controlled approximation, since these effects are essential in order to understand the behavior of these materials. In the past years there has been an enormous effort into improving this description by combining *ab-initio* calculations with many-body methods like the LDA+U (Local Density Approximation plus on-site U)¹ and the LDA+DMFT (Local Density Approximation combined with Dynamical Mean Field Theory)². While the original implementation of the Dynamical Mean Field theory was based on a single-band model, most compounds of interest involve more than one correlated orbital. This calls for the need of a multi-orbital extension of the LDA+DMFT technique. Recently, a new implementation of the multi-orbital LDA+DMFT has been proposed which uses the localized Wannier functions generated by the N-th order muffin-tin-orbital (NMTO) method³ in order to construct the LDA Hamiltonian and solves the many-body problem by DMFT including the non-diagonal contribution of the on-site self-energy. Such approach has been found to be highly successful in a series of recent applications^{4,5,6}. We will consider this procedure here in order to unveil the electronic properties of the layered Mott insulator TiOCl.

TiOCl, which consists of bilayers of Ti³⁺ and O²⁻ parallel to the *ab* plane, separated by layers of Cl⁻ ions stacked along the *c*-axis (see Fig. 1) has recently raised a lot of discussion due to its puzzling behavior at moderate to low temperatures. Large phonon anomalies have been observed in Raman measurements⁷ at temperatures around 135K as well as temperature-dependent *g*-factors and line-widths in ESR⁸. The susceptibility measurements⁹ show a kink at $T_{c2} = 94$ K and an exponential drop at $T_{c1} = 66$ K, indicating the opening of a spin-gap which is accompanied by a doubling of unit-cell along the *b*-axis¹⁰. While phonons are undoubtedly playing an important role in the behavior of this system, electron correlation is fundamental in order to understand these anomalous properties and we will here concentrate on the electronic description.

Recent electronic structure calculations of TiOCl within the framework of LDA+U^{9,11} for the crystallographic data at $T > T_{c2}$ show that in this temperature range the ground state of the system is described by chains of Ti ions along the *b*-direction (see Fig. 1) with the 3*d* electrons occupying the d_{xy} orbitals. Such a study¹¹ further revealed the importance of the phonon degrees of freedom at temperatures $T > T_{c2}$ by pointing out that certain A_g phonon modes consistent with the *Pmmn* space group of the high temperature structure may lead to orbital fluctuations with the ground state switching from d_{xy} to d_{yz}/d_{xz} . However, the implementation of LDA+U calculations¹² involves the assumption of a particular spin ordering in the system, which is fictitious since there is no true long range order in TiOCl. This makes the comparison of the LDA+U derived DOS with the experimentally measured photo-emission data doubtful. Also, LDA+U being a mean-field method, treats the correlation effects beyond LDA in a mean-field sense and suppresses all the fluctuation effects. For early transition metal oxides like titanates which are moderately correlated systems such fluctuation effects can turn out to be essentially important. One ingenious way of treating the dynamical fluctuation effects, is the DMFT which - though it freezes the spatial fluctuations- takes fully into account the temporal fluctuations. In the present communication, we aim to study the electronic structure of the high temperature ($T > T_{c2}$) phase of TiOCl by means of the NMTO+DMFT method.

Methodology -

The octahedral crystal field provided by the O₄Cl₂ octahedron, surrounding the Ti site splits the five degenerate *d*-orbitals into t_{2g} and e_g manifolds. The Ti³⁺ ion, in a 3*d*¹ configuration, therefore fills 1/6-th of the t_{2g} complex, leaving the e_g complex empty. The basic LDA electronic structure was reported in Ref.^{9,11}. The essential features involve Cl and O-*p* dominated bands extending from about -8 to -4 eV, separated by a gap of about 2.5 eV from the Ti-*d* complex, with the zero of energy set at the Fermi level. The Ti- t_{2g} bands cross the Fermi level with a tiny gap of about 0.2 eV between the occupied t_{2g} manifold and unoccupied e_g manifold.

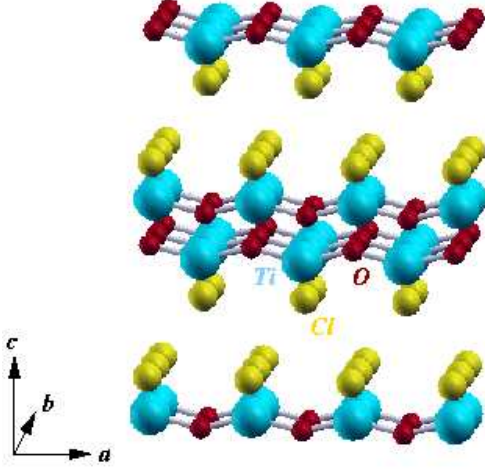


FIG. 1: Layered structure of TiOCl crystal. Two O atoms from the same layer and two O and two Cl atoms from neighboring layers form the O_4Cl_2 octahedra surrounding the Ti atom.

The TiOCl system can therefore be described by a low-energy, multi-band Hubbard Hamiltonian,

$$H = H^{LDA} + \frac{1}{2} \sum_{imm'\sigma} U_{mm'} n_{im\sigma} n_{im'\sigma} \quad (1)$$

$$+ \frac{1}{2} \sum_{im(\neq m')\sigma} (U_{mm'} - J_{mm'}) n_{im\sigma} n_{im'\sigma}$$

where $n_{im\sigma} = c_{im\sigma}^\dagger c_{im\sigma}$ and $c_{im\sigma}^\dagger$ creates a σ -spin electron in a localized t_{2g} orbital (m) at site i . H^{LDA} is the one-electron Hamiltonian given by LDA. We assume double counting corrections to be orbital-independent within the t_{2g} manifold, thus resulting into a simple shift of the chemical potential. The many-body Hamiltonian defined in Eq. 1 depends on the choice of the localized orbitals. In the present calculation, we employed the NMTO³ method for defining these localized orbitals. In this method, a basis set of localized orbitals is constructed from the exact scattering solutions of a superposition of short-ranged, spherically-symmetric potential wells (the so-called muffin-tin approximation to the potential) at a mesh of energies, $\epsilon_0, \epsilon_1, \dots, \epsilon_N$. The number of energy points, N , defines the order of such muffin-tin orbitals, the NMTO's. Each NMTO satisfies a specific boundary condition which provides it with an orbital character and makes it localized. The NMTO's being energy-selective in nature are flexible and may be chosen to span selected bands. If these bands are isolated -as is in the case of t_{2g} -derived bands in TiOCl- the NMTO set spans the Hilbert space of the Wannier functions. In other words, the orthonormalized NMTO's are the localized Wannier functions. In our example of TiOCl, the low-energy Hamiltonian defined in Eq. 1, involves only three correlated, localized t_{2g} Wannier orbitals and no

other orbitals. However, for such Wannier functions to be complete, they must involve contributions from the other degrees of freedom, *e.g.* O- p and Cl- p . This is achieved via the *downfolding* procedure³ which adds on to Ti centered t_{2g} orbitals, tails with O- p and Cl- p character, thereby defining an effective set of t_{2g} orbitals. It is important to note here, that the choice of the orbital symmetries $d_{xy}, d_{yz}, \dots, d_{3z^2-1}$ depends on the choice of the co-ordinate system. Throughout this paper and also in previous work^{9,11}, the choice has been made as $\hat{z} = a$, and \hat{x} and \hat{y} axes rotated 45° with respect to b and c . However, due to the distorted geometry of the TiO_4Cl_2 octahedra, the chosen co-ordinate system differs from the local co-ordinate system and the various d orbitals defined following the above mentioned co-ordinate system are not the exact eigenstates of the on-site Ti- d Hamiltonian. This introduces mixing between the t_{2g} and e_g symmetries. The t_{2g} NMTO's therefore, contain also the on-site and tail e_g character. For a realistic description of the LDA contribution and for the proper description of the localized orbitals in Eq. 1 it is essential to consider these issues. To our knowledge, so far no other LDA+DMFT is capable of taking these contributions into account properly. The plot of such Wannier functions is shown in Ref.¹¹.

In Fig. 2, we show the off-diagonal part of the 3×3 density matrix constructed out of the effective, downfolded t_{2g} NMTO's:

$$N_{mm'} = \sum_{k,n} u_{k,n}^m \delta(E - E_n, k) u_{k,n}^{m'}$$

$m, m' = 1, 2, 3$ refer to t_{2g} orbitals at the same site and $u_{k,n}^m$ are the appropriate normalized eigenvectors for the downfolded t_{2g} bands in the orthonormalized NMTO basis. The summation over k runs over all the k -points in the Brillouin zone (BZ) and n runs over all the t_{2g} bands. As is seen from the plot, it has non-negligible off-diagonal elements within the chosen co-ordinate system.

The DMFT² maps the many-body crystal problem defined in Eq. 1 onto an effective, self-consistent, multi-orbital quantum impurity problem. The corresponding local Green's function matrix is calculated via the BZ integration,

$$G(\omega_n) = \sum_k [(\omega_n + \mu)I - H^{LDA}(k) - \Sigma(\omega_n)]^{-1} \quad (2)$$

where μ is the chemical potential defined self-consistently through the total number of electrons, $\omega_n = (2n + 1)\pi/\beta$ are the Matsubara frequencies with β as the inverse temperature ($\beta = 1/T$). Σ is the self-energy matrix.

In our DMFT implementation we consider all components of the self-energy matrix $\Sigma_{mm'}$ between different t_{2g} Wannier functions at a given Ti site, including the off-diagonal contribution. The importance of these off-diagonal elements has already been inferred from the

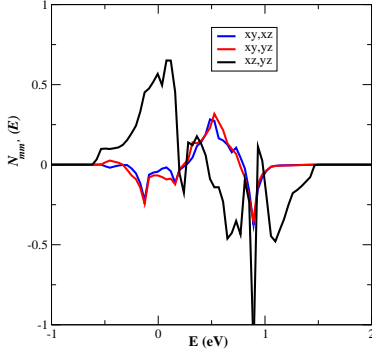


FIG. 2: Off-diagonal matrix elements of t_{2g} LDA DOS matrix (states/eV) in the Wannier representation.

plot shown in Fig. 2. This is in contrast to earlier LDA+DMFT implementations¹³ where it was assumed that the on-site block of the single-particle Green's function is diagonal in the space of the localized orbitals defining the many-body Hamiltonian. While such an approach is exact for the materials with perfect cubic symmetry, it becomes an approximation for materials having distortions.

The self-consistency condition within DMFT implies the local Green's function to be the same as the corresponding solution of the quantum impurity problem $G_\sigma(\tau - \tau') = 1/Z \int D[\mathbf{c}, \mathbf{c}^\dagger] e^{-S_{eff}} \mathbf{c}(\tau) \mathbf{c}^\dagger(\tau')$, where the effective action S_{eff} is defined in terms of the so-called bath Green's function $\mathcal{G}_\sigma^{-1}(\omega_n) = G_\sigma^{-1}(\omega_n) + \Sigma_\sigma(\omega_n)$, which describes the energy, orbital, spin and temperature dependent interaction of a particular site with the rest of the medium,

$$\begin{aligned}
 S_{eff} = & - \int_0^\beta d\tau \int_0^\beta d\tau' Tr[\mathbf{c}^\dagger(\tau) \mathcal{G}_\sigma^{-1}(\tau, \tau') \mathbf{c}(\tau')] \\
 & + \frac{1}{2} \sum_{imm'\sigma} U_{mm'} n_{im\sigma} n_{im'\sigma} \\
 & + \frac{1}{2} \sum_{im(\neq m')\sigma} (U_{mm'} - J_{mm'}) n_{im\sigma} n_{im'\sigma}
 \end{aligned}$$

$\mathbf{c}(\tau) = [c_{im\sigma}(\tau)]$ is the super-vector of the Grassman variables and Z is the partition function. The multi-orbital quantum impurity problem is solved by the numerically exact Quantum Monte Carlo (QMC) scheme. Standard parametrization¹⁴ has been used for the direct and exchange terms of the screened Coulomb interaction, $U_{mm'}$ and $J_{mm'}$ with $U_{mm} = U$, $U_{mm'} = U - 2J$ and $J_{mm'}(\neq m) = J$. For our calculation we have used $U = 4$ eV and $J = 0.5$ eV, which are reasonable choices for an early transition metal like Ti¹¹. The computational effort becomes prohibitive rather quickly as one lowers the temperature since in order to maintain the accuracy of the calculation one needs to increase the imaginary time slices as one increases β . The results reported in the fol-

lowing are done for $\beta = 20$ (T = 580 K) with 100 slices in imaginary time and 10^6 QMC sweeps. The maximum entropy method¹⁵ has been used for analytical continuation of the diagonal part of the Green's function matrix to the real energy axis to get the DMFT spectral density.

In this context, recently a LDA+DMFT calculation has been reported for TiOCl¹⁶. The calculation scheme in Ref.¹⁶ is based on a multi-orbital generalization of the iterated perturbation theory (IPT) for impurity solver. We consider the NMTO+DMFT scheme to be superior to the IPT approximation for the present problem. The multi-orbital QMC solver gives an accurate solution of the correlated orbitally polarized nonmagnetic t_{2g} problem, while the IPT scheme, which is very successful for the one-band DMFT problem² becomes quite uncertain in the anisotropic multi-band case¹⁷.

LDA+DMFT results and discussions -

Fig. 3 shows the orbital-resolved and total spectral functions obtained using the above explained LDA+DMFT technique, in comparison with the LDA total DOS. Consideration of the correlation effect beyond LDA within the framework of DMFT opens up a gap of ≈ 0.3 eV between the occupied and unoccupied spectra, signaling the insulating nature of the compound while the LDA DOS shows the finite density of states at the Fermi energy. We also note the appreciable broadening of the bandwidth in LDA+DMFT compared to the LDA bandwidth due to the redistribution of the spectral weight following the opening of the gap. The occupied bandwidth obtained in our LDA+DMFT calculation is in good agreement with recent photo-emission measurements¹⁸ which is about 2.5-3 eV. IPT-based LDA+DMFT calculations¹⁶ gave a bandwidth of 1.5-2 eV.

The on-site matrix elements of the tight-binding representation of the downfolded t_{2g} Hamiltonian in the NMTO Wannier function basis show that the d_{xy} orbital energy is about 0.4 eV lower than the d_{xz} and d_{yz} orbital energy, which are degenerate within the chosen co-ordinate system. This splitting is much smaller than the total t_{2g} bandwidth of the LDA DOS which is about 2 eV and is also smaller than the individual bandwidths of d_{xy} and d_{yz}/d_{xz} . As a consequence, in the LDA DOS the d_{xy} orbital is occupied by only 0.49 electron with the rest occupying the d_{xz} and d_{yz} orbitals. Turning to the LDA+DMFT results, the occupation matrix shows that the d_{xy} orbital becomes nearly full in contrast to LDA. The d_{xy} orbital is found to contain 0.98 electrons. The sharp increase in orbital polarization compared to the LDA result is in conformity with similar LDA+DMFT studies in LaTiO₃ and YTiO₃⁴, but is in contrast to IPT-based LDA+DMFT calculations for TiOCl which report¹⁶ non-negligible inter-orbital mixing, with 70% of the electrons residing in the d_{xy} .

As mentioned already, the gap value obtained in our calculation is about 0.3 eV, while the gap extracted from the optical conductivity data is about 1 eV in reflectivity

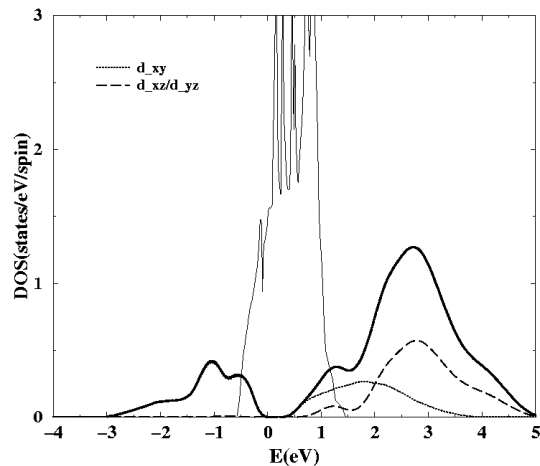


FIG. 3: DMFT spectral function at $T = 580\text{K}$ (thick line) and the LDA DOS (thin line). $\mu = 0$. The d_{xy} and d_{yz}/d_{xz} contributions are shown with dotted and dashed lines respectively. The spectral weight of the broad valence states is contributed almost entirely by d_{xy} .

experiments¹⁹ and 2 eV in transmittance experiments²⁰, the later being claimed as more sensitive for the gap determination²¹. As mentioned earlier, our QMC-DMFT calculations were carried out at a temperature, $T = 580\text{ K}$, while the experimental measurements were carried out at room temperature ($\approx 300\text{K}$) and below. Recent work on V_2O_3 ²² shows the successive filling of the Mott-Hubbard gap on raising the temperature. Therefore, the use of temperatures higher than room temperature may be a cause of the underestimation of the gap value obtained in the theoretical result. Nevertheless, it is hard

to justify such a large discrepancy as merely a temperature effect. The IPT-based DMFT calculations which claim²³ to achieve significantly lower temperatures than the QMC-DMFT calculations, predict for TiOCl (with $U=3.3\text{ eV}$ and $J=1\text{ eV}$) a gap which is less than 0.5 eV ¹⁶. The only way to reproduce a gap value as large as $\approx 2\text{ eV}$, within the single-site DMFT scheme, seems to be to use an unreasonably high U value. We therefore suspect that a major contribution to this discrepancy is caused by the neglect of the component of the self-energy between different sites, *i.e.* by the single-site approximation of the DMFT. The dimerization of the crystal and formation of spin-singlet bonds at low temperature below the ordering temperature can have a precursor at high temperatures in form of a short-range ordering effect, resulting into formation of dynamical Ti-Ti singlet pairs²⁴. Consideration of such effects is beyond the scope of the single-site DMFT since one needs to consider at least a cluster of 2 Ti sites to capture these features. Experience with VO_2 ⁶ already indicates that such effects can be extremely important in widening up the band gap. We intend to consider the cluster DMFT for TiOCl in our forthcoming communication. We mention here that the phonon effects could be important as well, as already found in connection with orbital fluctuations,¹¹ leading to additional smearing of the spectral features which is probably seen in the experimental PES data¹⁸.

Acknowledgments. - We would like to thank R. Claessen for discussing his results with us prior publication as well as P. Lemmens and M. Grüninger for useful comments. One of us (R. V.) thanks the German Science Foundation for financial support.

- ¹ V. I. Anisimov, J. Zaanen, O. K. Andersen, Phys. Rev. B **44**, 943 (1991).
- ² see for a review A. Georges, G. Kotliar, W. Kraut, M. J. Rozenberg, Rev. Mod. Phys. **68**, 13 (1996).
- ³ O. K. Andersen and T. Saha-Dasgupta, Phys. Rev. B **62**, 16219 (2000); Bull. Mater. Sci. **26**, 19 (2003).
- ⁴ E. Pavarini *et al.*, Phys. Rev. Lett. **92**, 176403 (2004).
- ⁵ A. I. Poteryaev, A. I. Lichtenstein and G. Kotliar, Phys. Rev. Lett. **93**, 086401 (2004).
- ⁶ S. Biermann, A. I. Poteryaev, A. I. Lichtenstein and A. Georges, *cond-mat/0410005*.
- ⁷ P. Lemmens, K. Y. Choi, G. Caimi, L. Degiorgi, N. N. Kovaleva, A. Seidel, and F.C. Chou, Phys. Rev. B **70**, 024506 (2004).
- ⁸ V. Kataev, J. Baier, A. Möller, L. Jongen, G. Meyer, and A. Freimuth, Phys. Rev B **68**, 140405 (2003).
- ⁹ A. Seidel, C. A. Marianetti, F. C. Chou, G. Ceder, and P. A. Lee, Phys. Rev. B **67**, 020405 (2003).
- ¹⁰ M. Shaz, S. van Smaalen, L. Palatinus, M. Hoinkis, M. Klemm, S. Horn, R. Claessen, *preprint*
- ¹¹ T. Saha-Dasgupta, R. Valentí, H. Rosner and C. Gros, Europhys. Lett. **67**, 63 (2004).
- ¹² V. I. Anisimov, F. Aryasetiawan and A. I. Lichtenstein, J.

- Phys.: Condens. Matter **9**, 767 (1997).
- ¹³ K. Held, I. A. Nekrasov, N. Blümer, V.I. Anisimov and D. Vollhardt, Int. J. Mod. Phys. B **15**, 2611 (2001).
- ¹⁴ R. Fresard and G. Kotliar, Phys. Rev. B **56**, 12 909 (1997).
- ¹⁵ For a review on the maximum entropy method see M. Jarrell and J. E. Gubernatis, Physics Reports **269**, 133 (1996).
- ¹⁶ L. Craco, M. S. Laad and E. Müller-Hartmann, *cond-mat/0410472*.
- ¹⁷ A.I. Lichtenstein and M.I. Katsnelson, Phys. Rev. B **57**, 6884 (1998).
- ¹⁸ R. Claessen *et al.*, *to be published*.
- ¹⁹ G. Caimi, L. Degiorgi, N.N. Kovaleva, P. Lemmens, and F.C. Chou, Phys. Rev. B **69**, 125108 (2004).
- ²⁰ C. H. Maule *et al*, J. Phys. C: Solid State Phys. **21** 2153 (1988).
- ²¹ M. Grueninger, *private communication*.
- ²² S. -K. Mo *et al.*, Phys. Rev. Lett. **93** 076404 (2004).
- ²³ L. Craco *et al.* *cond-mat/0309370*.
- ²⁴ The signature of such dynamical fluctuation is already evident in the angle resolved photo-emission spectra from R. Claessen's group.